Phase shift monitoring of delay-line interferometer and its application in phase-shift keying signal system

He Wen (闻 和)*, Jinxin Liao (廖全鑫), Xiaoping Zheng (郑小平), Hanyi Zhang (张汉一), and Yili Guo (郭奕理)

State Key Laboratory on Integrated Optoelectronics/Tsinghua National Laboratory for Information Science and Technology, Department of Electronic Engineering, Tsinghua University, Beijing 100084, China

**Corresponding author: wen-he@tsinghua.edu.cn*

Received October 20, 2011; accepted January 18, 2012; posted online March 15, 2012

The relation between the phase shift and the mean optical power (MOP) output from a delay-line interferometer (DLI) port applied for phase-shift keying (PSK) signal demodulation is proven of a cosine law irrelevant to signal modulation condition. The variation amplitude of the MOP is proportional to the transition duration of the modulation pulses. This phenomenon is interpreted as the result of the statistical and waveform characteristics of the PSK. The conclusions verified by simulation and experiment are generalized to other modulation formats and then applied to phase detuning monitoring, delay time judgment of DLI, and independence of modulation data assessment.

OCIS codes: 060.5060, 120.3180, 070.1170.
doi: 10.3788/COL201210.070601.

Delay-line interferometer (DLI) has been widely used in optical communication to demodulate phase-shift keying (PSK) signal for direct detection by converting the optical phase information to amplitude[1,2]. The phase shift of DLIs greatly affects the quality of the demodulated signal, that is, minor phase shift detuning results in an eye opening closing, lowered noise tolerance, and increased bit error ratio (BER)[3,4]. These deteriorations become more severe in the case of multi-level modulation formats. The tolerable phase shift detuning effects at a 1-dB optical signal-to-noise ratio (OSNR) penalty are about 16° and 6° for differential PSK (DPSK) and differential quadrature PSK (DQPSK) formats, respectively[4]. Such a stringent requirement puts a great challenge on the design, manufacturing, and packaging of the DLI-based demodulators. Precise temperature control combined with athermal package is required to stabilize the phase shift[5]; however, long term stabilization cannot be guaranteed due to device aging and control circuit operation drifting. Consequently, an effective way for phase shift detuning monitoring is necessary.

Some proposed approaches include the engineering-oriented BER monitoring[6], optical frequency dithering[7,8], phase dithering[9], pilot insertion[10,11], and two-dimensional waveform analysis[12]. However, they are more or less inefficient or unpractical. The BER approach needs a forward error correction module operating at the bit rate, which is difficult for high data rate. Moreover, this approach is unable to differentiate the mixed impairments induced by many factors, such as chromatic dispersion (CD), polarization mode mode dispersion (PMD), and noise. The frequency dithering cannot be applied to the modules manufactured by different vendors as they obey different private protocols. Pilot insertion demands a change of the current transponder structure. Meanwhile, the perturbation-free schemes are preferred for its simplicity and adaptability.

In this letter, we treat the PSK signal itself as a probe signal, through which we study the influence on the output signal given by DLI phase shift detuning. The mean optical power (MOP) output from one DLI port varies with the phase shift in the form of a cosine, which is irrelevant to signal modulation condition and accumulated CD. This phenomenon is the result of the statistical and waveform characteristics of the PSK signal. After performing model analysis, simulation and experimental verification, we find that the amplitude of the power variation is mainly determined by the transition edge of the driving signal pulse. With this conclusion, we can perform DLI phase shift detuning monitoring and delay time judgment in a simple but effective way.

First, we obtained the relation between the phase shift and the MOP output from one DLI port, using the transfer functions of a Mach-Zehnder modulator (MZM) and DLI. We assumed that the signal driving MZM was bipolar, with both polarities having identical probability; each channel of the signal was independent identically distributed (IID), and the pulse shape of the signal was approximated as a trapezoid. The detected MOP is expressed as

$$\begin{aligned} P(\phi,\tau) &\propto \lim_{T\to\infty}\frac{1}{4T}\int_0^T \left|E(t)+E(t+\tau)\,\mathrm{e}^{\mathrm{j}\phi}\right|^2 \mathrm{d}t \\ &= \frac{1}{2}\left\langle |E(t)|^2\right\rangle + \frac{1}{2}\left\langle x(t)\,x(t+\tau)+y(t)\,y(t+\tau)\right\rangle \\ &\quad\cdot\cos\phi+\frac{1}{2}\left\langle x(t+\tau)\,y(t)-x(t)\,y(t+\tau)\right\rangle\sin\phi, \quad (1) \end{aligned}$$

where $E(t)$ is the electric field of the PSK signal; $x(t), y(t) = \sqrt{1-r}\cos[V_{\mathrm{b}\_x,y} + m_{x,y}\sum_{k=-\infty}^{\infty} h(kT_0)\,I_{x,y}\cdot(t-kT_0)]\pi/2V_\pi$ are the in-phase (I) and quadrature (Q) components of the PSK signal, respectively, which are generated by the two sub-MZMs in a dual-parallel MZM (DP-MZM) shown in Fig. 1; r is the power distribution factor of the quadrature component with a value ranged in $0\leqslant r\leqslant 1$; $V_{\mathrm{b}\_x,y}$ and $m_{x,y}$ are the DC biases and modulation depths of the two sub-MZMs, respectively; V_π is the half-wave voltage of the MZMs; $h(t)$ is the system

impulse response, which is approximated as a trapezoidal pulse with a single-side transition edge of η shown in Fig. 1; $I_{x,y}(t\text{-}nT_0)$ represents an information bit sequence taking a value of either 1 or –1; φ and τ are the phase shift and time delay between the two arms of the DLI, respectively; the symbol $<\ >$ denotes an averaging operation over time like $\langle x(t)\rangle = \lim_{T\to\infty}\int_0^T x(t)\,\mathrm{d}t \Big/ T$. The time required for averaging is determined by the optical power meter, often in microsecond magnitude that is fast enough to trace the phase drifting and long enough to average the variation of modulation signal.

Equation (1) indicates that the detected MOP varies with the phase shift changing trigonometrically, in which the amplitude of the cosine item is proportional to the summation of the self-correlations of the I and Q components, whereas the counterpart of the sine item is proportional to the difference between the cross-correlations of these two components. If the probability of the transition from one symbol to another is equal to its reversal, the time-averaged amplitude of the sine item approaches zero as it is an odd function of the time delay τ. However, due to the waveform characteristics, the time-averaged amplitude of the cosine item is not zero. In the following, we prove this by taking examples of non-return-to-zero (NRZ) DPSK and NRZ-DQPSK modulation format.

For the NRZ-DPSK format, r equals zero and there are four possible combinations of two adjacent bits with equal probabilities of 1/4, namely, (1, 1), (–1, –1), (1, –1) and (–1, 1). For the patterns of (1, 1) and (–1, –1), there is no transition between the adjacent two bits, hence, their contribution to the amplitude of the cosine item is given by

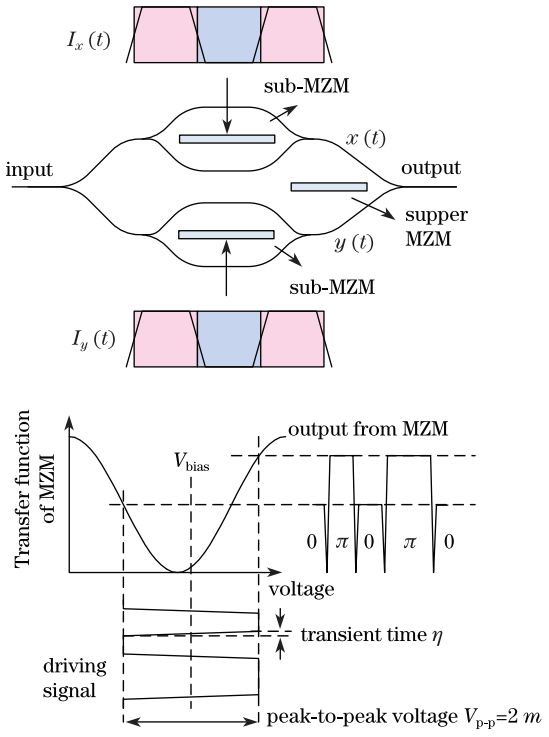

Fig. 1. Illustration of the NRZ-DQPSK generation through the application of dual-parallel MZM and trapezoidal pulse approximated driving signal.

$$f_1 = \frac{1}{8}\left\{\left[1-\frac{\eta}{2}\right]\left[1+\cos\frac{\pi(V_\mathrm{b}+m)}{V_\pi}\right] + \frac{\eta V_\pi}{\pi m}\sin\left(\frac{m\pi}{2V_\pi}\right) + \frac{\eta V_\pi}{\pi m}\left[\sin\frac{\pi(V_\mathrm{b}+m)}{V_\pi} - \sin\frac{\pi(V_\mathrm{b}+m/2)}{V_\pi}\right]\right\}. \quad (2)$$

In comparison, there is a transition for the patterns of (1, –1) and (–1, 1); thus, their contribution changes to

$$f_2 = \frac{1}{8}\left\{(1-\eta)\cos\left(\frac{m\pi}{V_\pi}\right) + \left(1-\frac{\eta}{2}\right)\cos\left(\frac{\pi V_\mathrm{b}}{V_\pi}\right) + \frac{\eta V_\pi}{\pi m}\left[\cos\left(\frac{\pi V_\mathrm{b}}{V_\pi}\right)\sin\left(\frac{m\pi}{V_\pi}\right) + \frac{3}{2}\sin\left(\frac{m\pi}{V_\pi}\right) - \sin\left(\frac{m\pi}{2V_\pi}\right)\right]\right\}. \quad (3)$$

Adding Eqs. (2) and (3), we derive the time-averaged amplitude of the cosine item and obtain a simplified result of $\eta/16$ if the NRZ-DPSK signal is generated perfectly in a condition of $V_\mathrm{b} = m = V_\pi$. In a similar way, we obtain the same result of the NRZ-DQPSK system in a condition of $V_{\mathrm{b}\_x,y} = m_{x,y} = V_\pi$.

Comparing the results of the NRZ-DPSK and NRZ-DQPSK systems, we find that they are similar, such that the cosine item is composed of two kinds of pattern contribution: the one with transitions giving a negative contribution and the other without transition giving a positive contribution. The effective power of the latter is slightly larger than that of the former due to the existence of the transition edges. Thus, the summation results in a positive value, which is proportional to the transition edge or the mean power difference between these two kinds of patterns. Given that the data of the I and Q channels are IID, the final results are the same for both systems. This conclusion can be generalized to other multi-level modulation formats if their generation is gained through the I/Q modulation, similar to that of the NRZ-DQPSK.

We performed both simulation and experiment to verify the above conclusion. In simulation, we generate the NRZ-DQPSK using a DP-MZM biased at the standard operation point, after which we allow the signal to pass through an ideal DLI with zero loss and a splitting ratio of 1:1. Varying the phase shift of the DLI, we recorded both the MOP and the demodulated signal eye diagram output from the same port of the DLI. In the experiment, we thermally heated one arm of the DLI made of 2 sliced 2 × 2 fiber couplers, and recorded the current passing through the thermal heater. The driving signal was a 10-Gb/s pseudo-random binary sequence (PRBS) signal with a length of $2^{31}-1$ bits.

Figure 2(a) presents the simulated relation between the phase shift and the MOP at the constructive port with a η of 0.3 bit slot, which varies cosinusoidally, with its maximum and minimum appearing at φ=0 and π, respectively. The demodulated eye diagrams at certain phase shifts, such as –180°, –135°, –90°, –45°, and 0°, are also listed in Fig. 2(b) as references for comparison with the experimental results.

The measured MOP varying with the heating current also approximates a cosine, shown in Fig. 3(a). We assume the phase shift of the DLI is proportional to the heating current in a certain extent. Some captured eye diagrams at certain heating current values

are also shown in Fig. 3(b), which agrees well with the simulated ones in terms of their occurring positions on the curve and the waveform details. The curve is not an ideal cosine because of the phase shift drifting of the DLI affected by environment variation during

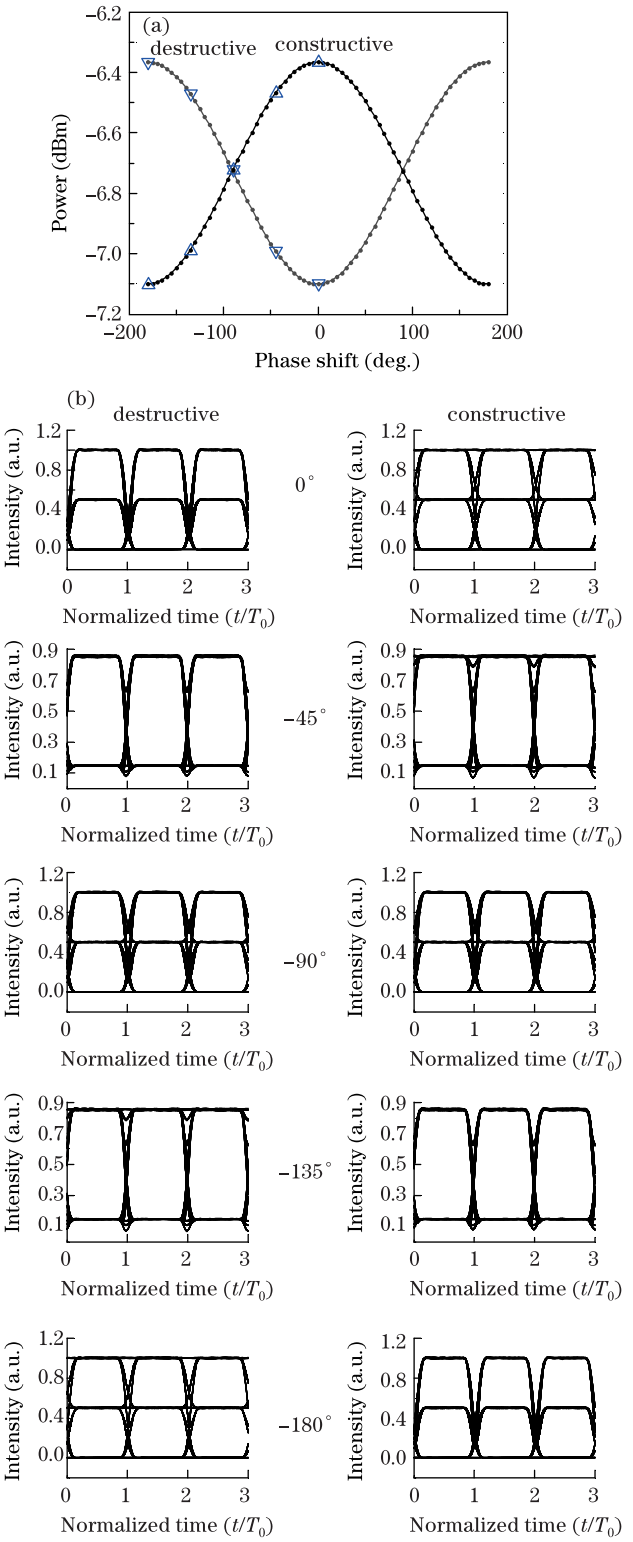

Fig. 2. (a) Simulated relation between the phase shift of DLI and the MOP output from one DLI port. (b) Differential demodulated signal eye diagrams of NRZ-DQPSK at certain phase shifts of DLI.

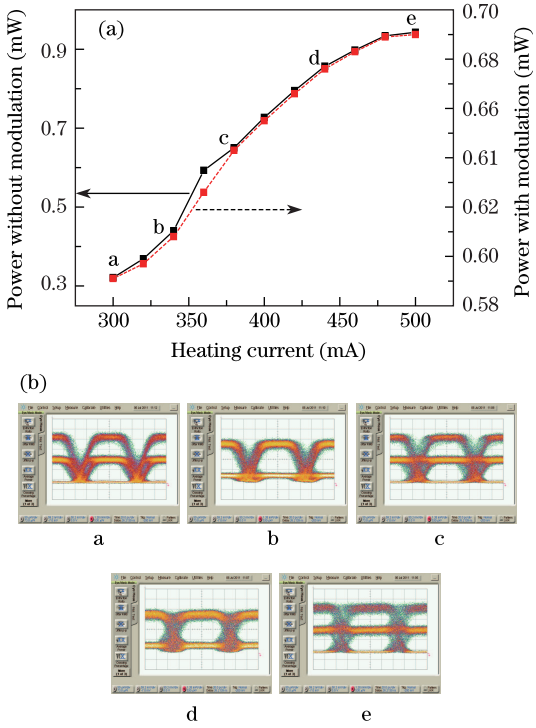

Fig. 3. (a) Heating current of DLI versus MOP output from one DLI port. (b) Differential demodulated signal eye diagrams of NRZ-DQPSK at certain heating current values.

measuring. Thus, this curve cannot estimate the phase shift accurately. However, it can be used to judge whether or not there is a phase detuning of a certain value. This is useful in the feedback control system, in which the accurate phase shift phase detuning can be controlled within a sufficiently small range determined by the sensitivity of MOP measurement. Despite the small variation of MOP, it was still detectable because there was a highly sensitive detection circuit in our experiment (such as a power meter with 4 effective digitals being accurate to 0.001 mW). To realize a phase shift accuracy of 6°, the required precision at the phase shift of $\pi/4$ is about $\eta/16 \sin(\pi/4)\,\Delta\phi \approx 0.0015$, or 0.3% relative variation (with a DC a little bit smaller than 0.5[13]). Thus, an ADC with resolution of 12 bits or more can meet such a requirement. The low sensitivity does not indicate ineffective, because the MOP is very stable or has some small uncertainty. On the contrary, if the measuring uncertainty is large, the high sensitivity would be useless.

Figure 4 shows the relation between the MOPs with application of driving signal and that without application at the same heating current. The MOPs were measured by switching the driving signal on and off with a short time interval so that the drifting of the phase shift became negligible. The linear relation indicates that the MOP varying with the phase shift follows the same strict cosine law, with the one free of phase modulation. This feature remains unchanged even if we alter the bias offset of the mother MZM in DP-MZM from –3.11 to –2.6 V, i.e., about 1/8 half-wave voltage, reduce the OSNR from 38 to 14 dB by noise loading, and distort the signal with dispersion amount of 400 ps/nm (Fig. 4). The results demonstrate the robustness of MOP monitoring. In general, for any unknown signal, if the modulation pulse

shape has similar property, such as the same ratio of transition edge to bit duration, the power ratio of the two PDs can be used to characterize DLI; this can then be recorded as reference in the system setup and tested without need for further scanning. However, if the ratio of transition edge to bit duration is changed induced by waveform distortion by dispersion, filtering the reference could not be used and rescanning would be required. This behavior is inherent in all the passive monitoring schemes that lack a known reference[12].

Both theoretical analysis and simulation results reveal that the amplitude of the cosine variation of the MOP is proportional to the transition edge of the driving pulse (Fig. 5). For the trapezoidal pulse, the scaling coefficient is 1/16, while for other types of pulses, the scaling coefficient is smaller than 1/16 due to the sharper transition edge. There is no difference between NRZ-DPSK and NRZ-DQPSK as expected. Despite the insensitivity of the MOP to phase detuning, it is stable and robust to other impairments (Fig. 4). Furthermore, sensitivity is raised when the delay time of the DLI is slightly shorter than one bit slot; this is because the partial overlap of the same symbol from both arms resulted in a positive increment of the signal self-correlation. Therefore, the MOP can be used to monitor the phase detuning even with low sensitivity.

This monitoring approach is preferred for at least three specific applications. First, it monitors the phase detuning in a DLI used for PSK signal demodulation. This is particularly true for the cases replacing inline dispersion compensation with electrical equalization[14], in which the signal is severely distorted by a large accumulated CD, resulting in the failure of other monitoring schemes based on waveforms[12]. In practice, we inserted another PD in front of the DLI to detect the power fluctuation and used the ratio of these two PD outputs to cancel out the effect of the power fluctuation. We emphasize that the proposed method is a simple way to monitor the phase detuning of DLI, although the method may have relatively poorer accuracy compared with the active monitoring schemes[8−11]. The proposed method is a passive monitoring scheme to estimate the unknown parameters in a random environment without using perturbation of a known signal. It is simple, adaptive to a wide range of applications, and has multiple functionalities. These features inherent in the passive monitoring schemes make them ideal for laboratory applications,

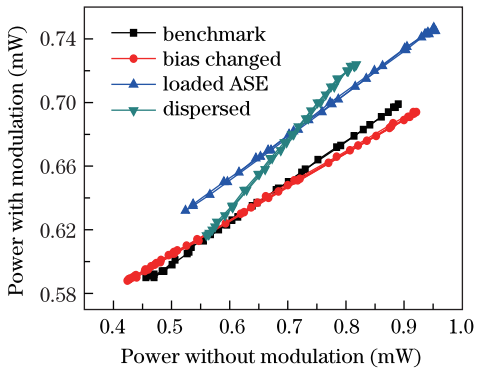

Fig. 4. Relation between the MOP with and without the application of driving signal under different conditions.

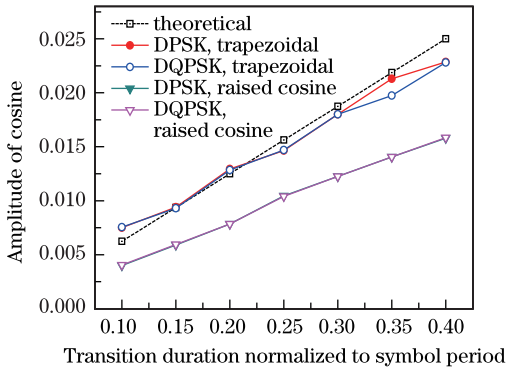

Fig. 5. Transition duration of different driving pulses versus the cosine amplitude of the MOP output.

such as judging whether or not there is phase shift drifting, in which we only care whether or not instead of how much.

Secondly, we can judge whether or not the delay time of a DLI is smaller than one bit duration according to the MOP variation amplitude, since the maximal amplitude is determined by the transition edge of the modulation pulse (Fig. 5). In our experiment, the MOP varies, with values larger than 0.67 dB (Fig. 3), even surpassing 0.54 dB ($10\log(0.5+0.5/16)-10\log(0.5-0.5/16)$), which is only achieved at a transition duration of η=0.5. By considering the real transition duration that is smaller than 0.5, the extra amount of MOP variation is attributed to the shorter than one bit duration delay time of DLI.

Finally, our proposed approach provides an effective way to test the statistical independence of the data between the I and Q channels, as well as the equal probability of each polarity of the bipolar data. If these conditions are not met, the relation between the phase shift and the MOP turns to a trigonometric function composed of both sine and cosine items. Therefore, the relation between the MOPs with and without application of the driving signal can degenerate from linear to elliptical.

In conclusion, we find and assess the fact that for direct detection of PSK, the MOP from one DLI port varies cosinely with the DLI phase detuning, whose amplitude is proportional to the transition edge of the driving signal pulse. This behavior can be used to monitor the phase detuning for its robustness to many impairments.

This work was supported in part by the National Natural Science Foundation of China (Nos. 61007045, 61025004 and 61032005), and the National "863" Program of China (Nos. 2009AA01Z223 and 2009AA01Z253).

References

1. A. H. Gnauck and P. J. Winzer, J. Lightwave Technol. **23,** 115 (2005).
2. H. Wen, J. Liao, X. Zheng, and H. Zhang, Chin. Opt. Lett. **9,** 100607 (2011).
3. H. Kim and P. J. Winzer, J. Lightwave Technol. **21,** 1887 (2003).
4. K.-P. Ho, IEEE Photon. Technol. Lett. **16,** 308 (2004).
5. F. Seguin and F. Gonthier, in *Proceedings of OFC2005* OFL5 (2005).

6. H. Haunstein and R. Schlenk, "Control of Delay Line Interferometer" U.S. Patent 7266311 (2007).
7. J. Li, K. Worms, D. Hillerkuss, B. Richter, R. Maestle, W. Freude, and J. Leuthold, in *Proceedings of OFC2010* JWA24 (2010).
8. J. Li, K. Worms, R. Maestle, D. Hillerkuss, W. Freude, and J. Leuthold, Opt. Express **19,** 11654 (2011).
9. H. Kawakami, E. Yoshida, Y. Miyamoto, M. Oguma, and T. Itoh, Electron. Lett. **44,** 437 (2008).
10. L. Christen, S. Nuccio, Y. K. Lize, N. Jayachandran, A. E. Willner, and L. Parschis, in *Proceedings of CLEO2007* CMJJ2 (2007).
11. H. C. Ji, P. K. J. Park, H. Kim, J. H. Lee, and Y. C. Chung, IEEE Photon. Technol. Lett. **18,** 950 (2006).
12. J. Zhao, A. P. T. Lau, C. Lu, H. Y. Tam, and P. K. A. Wai, IEEE Photon. Technol. Lett. **22,** 1018 (2010).
13. H. Wen, Y. Ge, H. Jiang, L. Han, X. Chen, X. Zheng, H. Zhang, and Y. Guo, Proc. SPIE **7136,** 713636 (2008).
14. M. S. Alfiad, D. van den Borne, F. N. Huaske, A. Napoli, A. M. J. Koonen, and H. de Waardt, J. Lightwave Technol. **27,** 4583 (2009).